Journal of Applied Remote Sensing

Integration of geographic information system and RADARSAT synthetic aperture radar data using a self-organizing map network as compensation for real-time ground data in automatic image classification

Mohammad Mostafa Kamal
Peter J. Passmore
Ifan D. H. Shepherd

Integration of geographic information system and RADARSAT synthetic aperture radar data using a self-organizing map network as compensation for real-time ground data in automatic image classification

Mohammad Mostafa Kamal,[a] Peter J. Passmore,[b] and Ifan D. H. Shepherd [c]

[a] University of Saskatchewan, Department of Geography, 117 Science Place, Saskatoon, SK, S7N 5C8 Canada
mohammad.kamal@usask.ca

[b] Middlesex University, School of Engineering and Information Sciences, The Burroughs, Hendon, London, NW4 4BT, United Kingdom
p.passmore@mdx.ac.uk

[c] Middlesex University, Business School, The Burroughs, Hendon, London, NW4 4BT, United Kingdom
i.shepherd@mdx.ac.uk

Abstract. The paper presents results of using advanced techniques such as Self-Organizing feature Map (SOM) to incorporate a GIS data layer to compensate for the limited amount of real-time ground-truth data available for land-use and land-cover mapping in wet-season conditions in Bangladesh based on multi-temporal RADARSAT-1 SAR images. The experimental results were compared with those of traditional statistical classifiers such as Maximum Likelihood, Mahalanobis Distance, and Minimum Distance, which are not suitable for incorporating low-level GIS data in the image classification process. The performances of the classifiers were evaluated in terms of the classification accuracy with respect to the collected real-time ground truth data. The SOM neural network provided the highest overall accuracy when a GIS layer of land type classification with respect to the depth and duration of regular flooding was used in the network. Using this method, the overall accuracy was around 15% higher than the previously mentioned traditional classifiers at 79.6% where the training data covered only 0.53% of the total image. It also achieved higher accuracies for more classes in comparison to the other classifiers.

Keywords: remote sensing, geographic information system, neural network, radarsat.

1 INTRODUCTION

For some time, cloud cover problems have hindered the use of conventional, remotely sensed data for mapping land cover and land uses in the wet season in tropical countries such as Bangladesh. The relatively recent availability of satellite-based Synthetic Aperture Radar (SAR) data has thus opened up many opportunities in these application areas. The possibility of all-weather, day-and-night operation, and the ability to penetrate through clouds and other features, gives SAR some advantages over the optical systems [1-4]. The availability of the spaceborne Synthetic Aperture Radar (SAR) data has provided the scope for mapping land use and land cover even in wet season cloudy conditions, and especially in a tropical region such as Bangladesh where much of the time cloud cover limits the use of optical remote sensing. Synthetic aperture radar (SAR) is an active imaging system, which uses microwave bands of the electromagnetic spectrum to generate images through the coherent processing of

Received 17 Jun 2009; accepted 30 Apr 2010; published 5 Jun 2010 [CCC: 19313195/2010/$25.00]

the scattering signals. Woodhouse [5] provides a useful conceptual model of different aspects of radar remote sensing. SAR relies on the fact that radar is an active system; that is, the system both transmits, and receives, its own signals. The imaging mechanism [6] relies on both system parameters (wavelength, polarization, incidence angle, resolution) and object parameters (complex dielectric properties, surface roughness, terrain geometry and surface and volume scattering), as both are responsible for the radar backscattering from which the images are derived. Because the features of a SAR image result from radar backscattering rather than the reflection of sunlight, one needs to be careful during interpretation about this difference between the SAR and optical systems.

Analysis of SAR imagery deals with the tone, texture, shape, size, pattern, and other characteristics of the image with respect to the ground information. Due to the SAR interaction with the target and the imaging process, the identification of features in the image becomes more difficult when the target feature is agriculture and natural land cover, and especially objects that change with time and weather conditions. Therefore, to achieve better accuracy in the SAR data classification, the field conditions need to be known at the time when the satellite is imaging the area; this is referred to as real-time ground truth data. The collection of ground truth data is frequently influenced by several factors, including geo-physical and seasonal condition of the area that limits accessibility, the aerial extent of the area, and the available resources. This tends to be an expensive, time consuming, and difficult process. Moreover, although a single SAR image may contain useful information for crop classification, low accuracy is typically obtained unless the region under consideration is characterized by just a few crop types, which are significantly different with respect to their microwave signatures [7]. Brisco and Brown [7] also cited several examples of using multiple SAR images of different dates for better crop identification because, as the crops grow and their canopy and structure changes, their backscatter characteristics also change. Furthermore, such change may be different from crop to crop, which is also useful information in time-series radar data.

In the current study, four SAR images of different dates over the crop-growing period were used to distinguish different crops. However, the number of images used increases the work and expense of real-time ground data collection. Again, many researchers [8-11] have presented various methods of ground data collection and have indicated that inappropriate ground data collection easily result in 'Ground lies' [12]. In addition, the inherent speckle in SAR imagery makes classification much more complex than for optical imagery, and there is a major trade-off to be made between speckle reduction and the preservation of data integrity. As a result of these limitations, it is still rarely possible to achieve 80% accuracy in the classification of existing land use/cover with traditional classification methods, even after vigorous input of an expert's knowledge about field conditions, and then only for a few classes as output.

Advances in computer technology and software techniques have made it possible to process large volumes of diverse data about the Earth and its environment. An increasing number of studies incorporate not only spectral data but also other spatial data such as forest maps, soil maps, and topographic information such as elevation, slope and aspect. All these have potential use in image processing and classification. However, further work is required to integrate such data, in the form of geographical information system (GIS) layers, in order to improve the automatic classification of radar images. Automatic classification would have the benefit of reducing dependency on skilled technician support, especially in operational processing where remote sensing images are used to support managers and decision making on a regular basis. It is common practice in satellite image classification to classify the image first, and then to integrate the other information such as GIS layers. Our intention is to explore the possibility of using existing GIS layers during segmentation, in a way that would reduce dependency on the amount of training by providing additional information during the process and keeping the initial accuracy at optimum level. These advantages are particularly

necessary for operational monitoring schemes, especially where the frequency of information collection is high or data are required at regular intervals, as is commonly the case in the monitoring of agricultural land use.

2 MOTIVATION

In remote sensing image classification, numerous approaches have been used with varying degrees of success. Despite considerable developments in recent years, the accuracy with which thematic maps may be derived from remotely sensed data is often judged to be too low for operational use [13-14]. Conventionally, classification has been mainly based on classical statistical methods and decision theory, such as the maximum likelihood (MLH), Mahalanobis distance (MHD) and minimum distance (MND) classification. These classifiers rely upon the assumption that the populations from which training samples drawn are normally distributed. This is not always the case for remote sensing data [15], and especially for SAR images. The maximum likelihood decision rule is possibly the most used supervised approach, which is based on the probability that a pixel belongs to a particular class. This method assumes that these probabilities are equal for all classes, and that the input bands have normal distributions. The Mahalanobis distance decision rule uses the covariance matrix in the equation. Variance and covariance are calculated so that clusters that are highly varied will lead to similarly varied classes, and vice versa. The minimum distance decision rule (also called spectral distance) calculates the spectral distance between the measurement vector for the candidate pixel and the mean vector for each signature.

Foody [16] noted that the conventional statistical classification techniques may not always be appropriate for mapping from remotely sensed data, and identified some interrelated problems. Firstly, a conventional parametric classifier assumes that the data are normally distributed. Secondly, a large training sample is required to define a representative sample that would be the source of descriptive statistics (e.g. mean, covariance) for the classifier. Typically, as recommended by Mather [17], the minimum training set size is some 10-30 times the number of discriminating variables (such as the number of wavebands in multi-spectral image or number of images in time series) per class. This indicates that a very large training set is required for mapping from multi-spectral or multi-date remotely sensed images and this runs contrary to a major goal of remote sensing, which is to extrapolate over a large area from limited ground truth data. Therefore, in the case of high-dimensional datasets, there may be a need to identify the optimal band combination for the classification; otherwise, the accuracy may decline with an increase in the number of discriminating variables. A third limitation of conventional techniques is that the classification can only make direct use of data acquired at a high level of measurement and cannot accommodate directional data directly. Furthermore, there may be useful discriminatory information available in GIS at a low level of measurement precision (e.g. nominal level soil map or other datasets on various land properties) or a directional component (e.g. slope or aspect data), which cannot be incorporated into traditional techniques. However, the inclusion of such data in the classification process could potentially increase the discrimination of classes and reduce load on the ground truth data.

The above discussion suggests that incorporation of other data from GIS for use in image classification would require an alternative processing approach, which does not entirely depend on the statistical parameters of the input data. One of the most recent advances made in remote sensing has been the application of Artificial Neural Networks (ANNs) in a wide range of applications and image analysis [18]. Classification is one of the main applications of neural networks in remote sensing, and ANNs have been used in supervised classification [19-20], unsupervised classification [21] and image segmentation [22-24]. Petersen et al. [25] reviewed 200 applications of ANNs in remote sensing, 30% of which were in image segmentation/classification with the remainder in pre-processing, compression, recognition,

understanding and optimisation of remotely sensed images. These applications mainly used feed-forward neural networks, Kohenen feature maps and Hopfield neural networks. Each type of network has different properties and consequently they vary in appropriateness for different applications. Feed-forward networks have been used widely for supervised image classification [20], Hopfield networks have been used in studies involving stereo matching and feature tracking [26], while Kohonen networks are self-organising and so are particularly attractive for unsupervised and semi-supervised classification. Pham and Bayro-Corrochano [27] suggested Kohonen's Self-Organising feature Map (SOM) as an alternative to supervised techniques. Better results in SOM for multi-temporal satellite image classification in comparison to other neural network have already been demonstrated by several studies [28-30]. Merenyi et al. [31] recommend SOM because it is relatively easy in training over the most frequently used backpropagation network, and suggest SOM for high dimensional data as used in hyperspectral image classification, especially for its capability to make good predictions based on only a small training sample.

3 METHODOLOGY

The study area is in the southwest coastal region of Bangladesh (Fig. 1). The study used four SAR images, acquired by the RADARSAT 1 satellite system, on four different dates in the wet season cropping period: 18 August, 11 September, 5 October, and 29 October 2001. (These images were originally collected for the study from the Centre for Environmental and Geographic Information Services (CEGIS) in Bangladesh.) The images were acquired in standard beam mode (S5) and processed in 25-meters per pixel resolution. A subset of the image covering a district of the region was used at this stage of the research. The images were pre-processed for calibration by the RADARSAT as supplied to CEGIS as Path Image Product, and were geometrically corrected and coded to prepare a set of multi-temporal images and overlay that with other GIS and field data.

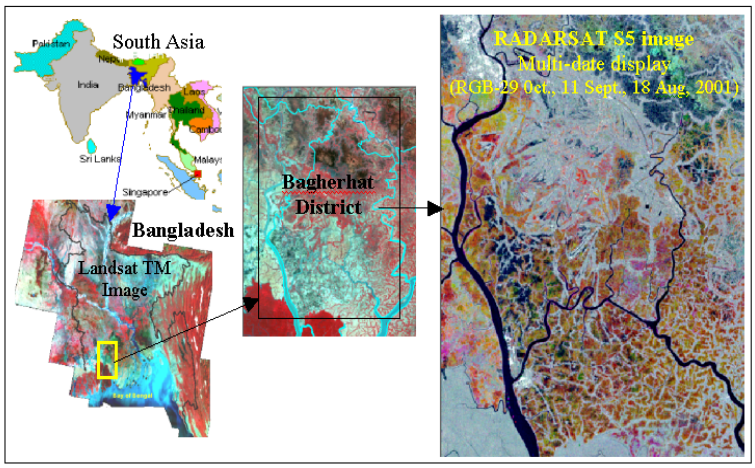

Fig. 1. Study area.

Images were obtained in dB (decibel) format. The subsequent processing steps for the images were co-registration, georeferencing, and then filtered using the Gamma-MAP filter [32]. It has been reported [33-34] that in Bangladesh the Gamma-MAP filter is best suited for SAR imagery, as commonly used by CEGIS. The co-registration among the images was undertaken using the ground control points (GCPs) method. Upon collection of the GCPs, the images were co-registered using the neighbourhood re-sampling technique to retain the integrity of the datasets. The co-registered radar images were compared with each other and less than 0.25 pixel root-mean-squares (RMS) error was obtained. The images were then

georeferenced to enable their subsequent use with GIS layers. Similar techniques were used for georeferencing the images where the GCPs were taken from the Differential Global Positioning System (DGPS) corrected Panchromatic image of the Indian Remote Sensing (IRS) satellite systems, and the same set of GCPs was used for all images.

Field information was collected in real time during image acquisition for all four imaging dates. The CEGIS field team, equipped with DGPS, field maps, camera and other instruments, collected information about the existing land cover condition for a number of land parcels in randomly chosen locations in the study area. Each of the land parcels was identified based on homogeneity of land cover and land uses. Information was collected on a pre-designed field data collection form. The main items of information collected were type of land cover and, in the case of vegetation or crops, current height, canopy, growth stage, presence of water and depth of water, height of plant over water, plantation time of crop and tentative harvesting time of crop. Geographic coordinates of two to four points for each of the parcels were recorded using DGPS. The land-parcels were identified on the GIS map using the location coordinates collected with DGPS to create polygon coverage. All collected information was converted and linked with the polygon coverage in the GIS. About half of the parcel information was used as training data in the image segmentation process, and the remainder was used as reference data for the evaluation of results. The same set of known pixels (from the field data) for the different classes was used for training or calibration for all the classifiers. The total number of training pixels was 0.58% of the total pixels in the image. The evaluation was also undertaken with the same set of known (reference) pixels, which is the other portion of ground truth data. The reference pixels comprised 0.47% of the total image pixels.

By analysing the field data and associated signatures in the temporal SAR images, 10 classes were identified for classification: Water, Grass, *B. Aman*, Rural settlements, Shrimp cultivation, Shrimp-*T. Aman*, *T. Aman*, Mangrove, Built-up area, and Unknown class. Figure 2 shows examples of these classes in which the images of the first, second and fourth dates have been assigned to the R, G and B channels respectively.) The major wet season land uses in the study area are the Shrimp and *T. Aman* rice cultivation. *T. Aman* is a transplanted High Yield Variety (HYV) rice paddy, for wet season growth, that is transplanted in the field after growing the broadcasted seedlings in seedbeds. However, the SAR signatures of any land-cover types are highly influenced by the inundation coverage and the canopy of the vegetation or crop floating or emerged over the water. These conditions highly influence the Grass, *B. Aman*, shrimp, and *T. Aman* areas. Table 1 provides a description of all land cover and land use classes.

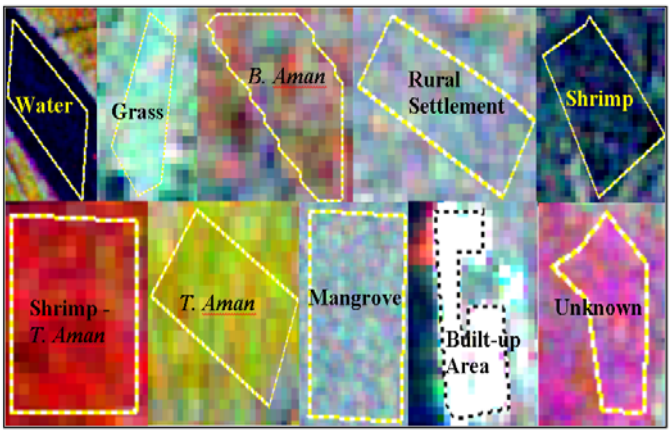

Fig. 2. Land-cover classes in the multi-temporal image.

A GIS layer 'Inundation Land Type' (land type) was also collected from the CEGIS for the study area. The Land-type [35] data are a combination of information for land level (which is derived from elevation data), flood inundation depth, and duration of inundation. The land type data layer is a national level raster GIS layer with 300-meter grid cell size and 1 to 11 cell values for land type categories. The data layer was re-sampled to 25-meters grid cell size to match the image cell size. It was then co-registered with the geo-referenced images so it could be used as an additional input vector in the Self-Organizing feature Map (SOM) neural network. The land type layer has only been used in the SOM network for the classification of the set of SAR images, as it is probably the most significant GIS layer that influences the vegetation and agricultural land cover [36] in Bangladesh.

The accuracy of the classifications was assessed based on the analysis of confusion matrices generated for all classifiers from the evaluation set of the ground truth data. The overall, user's and producer's accuracies and the Kappa coefficient [28] were calculated from the matrices. (The overall accuracy provides the probability of the correctness of the classes in the classified image, and the user's and the producer's accuracies provide impressions of the commission and omission errors respectively for each of the classes in the classified image.) The kappa coefficient calculated from the confusion matrices is preferred by many researchers, because the other indices are based on either of the principal diagonal, columns or rows of the matrix.

Image processing software (ERDAS Imagine) was used for pre-processing the data and for performing the MLH, MHD, and MND classification. Initially, the signature file was created using the training set of the ground truth data from the multi-temporal SAR images, and was used as the training/calibration data for all classifiers. The Self-Organizing feature Map (SOM) neural network developed by Kohonen [37] was used for integrating the land-type GIS layer. The review suggests that the capability of the automatic detection of relationships within the set of input patterns is useful in terms of the problem of image

Table 1. Description of the land cover and land use classes.

Class	**Description**
Water	Includes the field polygons containing clear water such as rivers, wetlands and other water bodies and provides a dark signature in the images for all dates.
Grass	Mainly grows in very low land areas that are inundated at the beginning of the wet season where HYV rice is cultivated only once a year during the dry season.
B. Aman	These are local deep-water variety of rice that grows in the medium low to lowlands areas, where rice are broadcasted in the field at the beginning of the wet season. The rice grows with the increase of water over time during the wet season.
Rural Settlements	Includes homesteads and associated vegetation and these are clearly identifiable patches in satellite images.
Shrimp	Includes both the saline (*Bagda*) and non-saline deep-water shrimp (*Golda*). The *Bagda* shrimp area, that are under year round cultivations are included in this category.
Shrimp & *T. Aman*	*Bagda* are cultivated only in the dry season and *T. Aman* rice is the following crop in the wet season. Transplantation of rice are delayed due the wait-time for flashing the salinity by the seasonal rain and the fresh water flow of the neighboring channels
T. Aman	Includes the fields with rice, which is transplanted from the beginning of the season (July-August).
Mangrove	The class is concentrated in the southern most part of the study area.
Built-up Area	The class mainly consists of urban centers and industrial zones, where there are very high backscattering in all images due to physical infrastructures in the landscape
Unknown	The class appears in a very distinct pattern in multi-temporal images, observed in some small pockets, and was not covered in the field data

mapping from higher dimensions to a two dimensional feature space. The SOM_PAK software from the Helsinki University of Technology was used for the SOM network classifications. Figure 3 shows the SOM network process using the SOM_PAK software. The

same training set of ground truth data that was used for preparing the class signatures for the statistical classifiers was used as the calibration data in SOM_PAK. Unlike most of the other neural networks, a SOM has no hidden layer but is composed of one input and one output layer.

The number of neurons in the input and output layer defines the SOM network. The

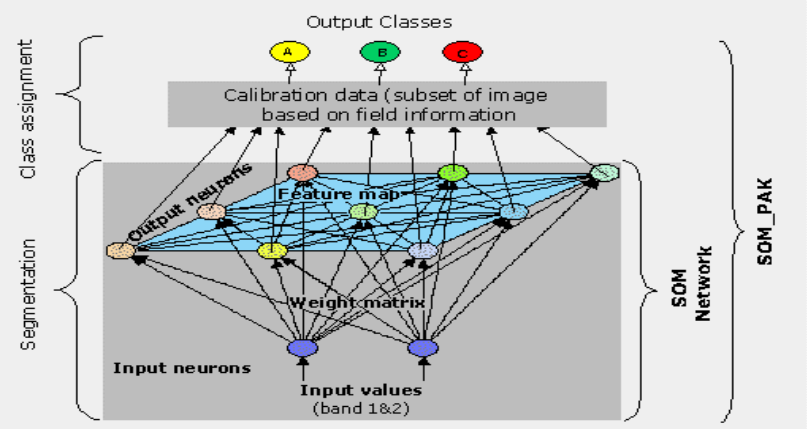

Fig. 3. SOM process in SOM_PAK.

number of input neurons is equal to the number of input vectors. In this study, the SOM network is tested for the classification of the previously mentioned multi-temporal SAR images both with and without the GIS layer. For the network used without the GIS layer, there were four input neurons for four images and the result is referred to as SOM4 in subsequent discussion. When the GIS layer was used in the network, then the input neurons were 5: 4 neurons for four images, and one for the GIS layer. This output is referred to as SOM5. However, there are no clear rules about the specification of the number of output neurons in the literature. The training and calibration data were also prepared accordingly. Several random combinations of number of output neurons, iteration, and other parameters were tested. Finally, a 10*12 output map was accepted with 100,000 iterations and hexagonal topology. The process took less than 5 minutes on a standard PC (Intel Pentium IV processor, Windows XP operating system) to process 5 layers of raster data, where each layer was 2130 by 1540 cells in size. The SOM_PAK software used for the SOM classification was unable to read the images and GIS data directly. Therefore, a conversion tool was developed using

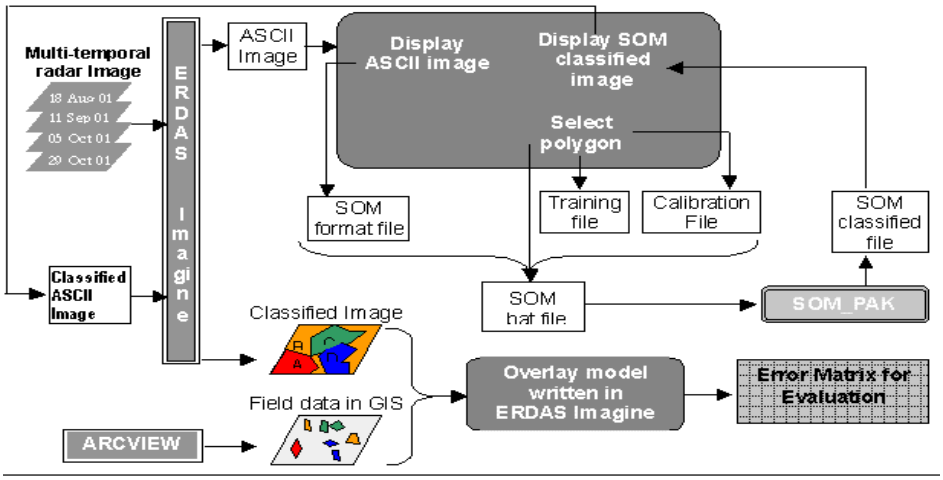

Fig. 4. Functionality of the conversion tool developed for classification.

Visual C++ for bi-directional data conversion between ERDAS Imagine and SOM_PAK. The ArcView GIS software was also used to prepare and convert the GIS field data for use as calibration data in SOM_PAK. Figure 4 illustrates the functionality of the SOM operation using SOM_PAK, the conversion tool, ERDAS Imagine, and the ArcView GIS software.

4 RESULTS

Table 2 provides the overall accuracy and kappa coefficient for all the classifications derived from the respective confusion matrices with respect to the ground truth data. This shows that the inclusion of the land-type layer (SOM5) as input to the SOM network substantially improves the accuracy of classification. In the absence of these data (SOM4) the worst overall accuracy and Kappa coefficient were achieved.

Table 2. Accuracy and Kappa coefficients of classifiers.

	Only multi-temporal SAR images				Images and Land-type
Classifier	MLH	MHD	MND	SOM4	SOM5
Overall Accuracy	64.71	63.36	65.64	58.19	79.57
Kappa coefficient	0.57	0.55	0.57	0.47	0.74

The classification results by different classifiers for a part of the study area (omitting SOM4) are shown in Figure 5. A visual inspection of the Fig. 5 suggests that in the MLH image, the Mangrove (shown in cyan) and the Settlements (shown in grey) are inter-mixed and the Settlements areas are misclassified as Mangrove across the entire image. In the MHD image, the Mangrove, Settlements, and the Grass (shown in green) classes are inter-mixed

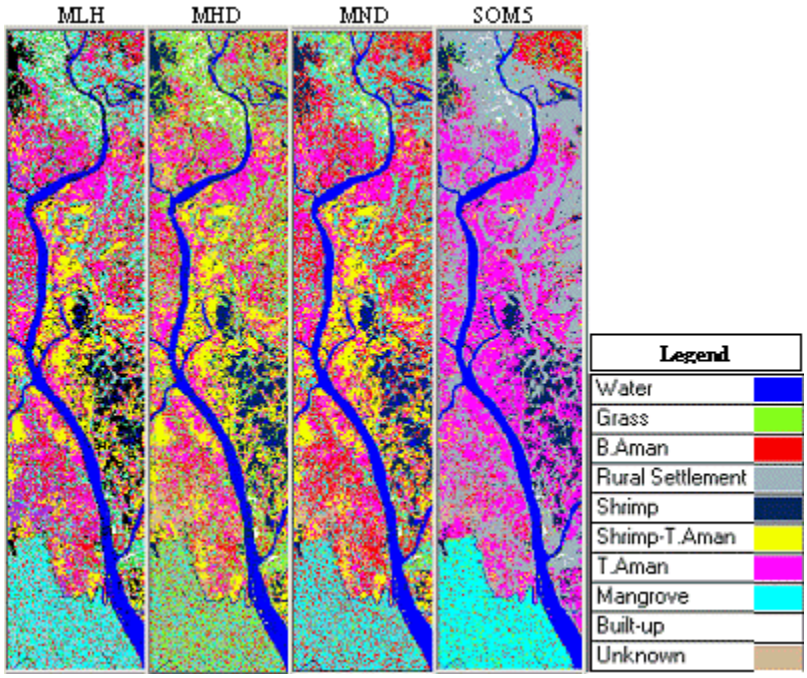

Fig. 5. Results of classifications by different classifiers.

and the Grass is dominating in this mix. In the MND image the condition of the Mangrove

and the Settlements classes are similar to the MLH image. The Grass and the *B. Aman* classes are identified more accurately in the MND image and far more accurately in the SOM5 image, lying in the upper-right corner, which is the correct location according to the field knowledge discussed above. The Settlement and the mangrove classes are clearly identifiable in SOM5. The 'Unknown' class also appears more clearly in the SOM5 image, as lying above the Mangrove area on the left hand side of the image. However, in terms of visual impression, the '*T. Aman*' class appears to be overestimated in SOM5 and to have recruited the area of 'Shrimp-*T.Aman*' class in comparison to the other methods. The Water, Built-up and Shrimp classes appear to be consistent in all of the classified images.

Table 3 provides the producer's and the user's accuracy respectively for each of the classes resulting from the different classifiers. From these data it is clear that none of the classifiers could maximise the user's and producer's accuracy for all of the classes. For example, the *T. Aman* class achieved the highest user's accuracy with MLH but the highest producer's accuracy with SOM5. The Shrimp & *T. Aman* class achieved the highest user's accuracy with the SOM5 but the highest producer's accuracy with MND. However, the user's and producer's accuracy of most of the classes were improved with the SOM5 classifier. For some classes the accuracies are very high (e.g. 97.9% for water with the MLH classifier), but for others they are low (e.g. only 18.7% for Shrimp & *T. Aman* with the SOM5 classifier). The accuracies for a particular class can go down with respect to other classifiers if the selection criterion is based on overall accuracy or Kappa values.

Table 3. User's and producer's accuracy.

Producer's accuracy (%)						User's accuracy (%)				
MLH	MHD	MND	SOM4	SOM5	Classes	MLH	MHD	MND	SOM4	SOM5
97.9	94.4	99.8	94.84	99.8	Water	96.9	97.4	95.7	99.97	97.5
38.4	61.5	29.3	50.59	47.6	Grass	66.7	40.3	67.8	4.30	74.6
40.7	27.8	48.7	10.56	69.6	B. Aman	13.4	11.7	12.1	28.26	27.6
33.9	45.7	38.8	0.00	96.2	Rural Settlements	46.4	49.5	48.3	0.00	76.2
53.7	58.4	42.6	58.28	43.6	Shrimp	47.6	40.7	58	34.18	58.8
61.2	60.6	61.8	17.89	18.7	Shrimp & *T. Aman*	18.6	19.1	21	64.48	44.4
26.9	29.3	33.4	87.13	61.5	T. Aman	89.5	88.4	88.4	30.65	78.3
63.6	19.6	52.7	25.04	86.3	Mangrove	44.2	50.4	44	85.18	78.6
100	100	96.2	0.00	97.4	Built-up Area	99.7	99.7	100	0.00	99.7
98.3	98.8	93.6	16.52	86.6	Unknown	32.9	29.7	37.6	38.19	42.2

5 DISCUSSION

The inclusion of the land-type GIS layer in the SOM network increased the overall accuracy by 15% over the other statistical classifiers. Out of the 10 land cover and land use classes, in SOM5, the user's accuracy increased for seven classes and the producer's accuracy increased for five classes, and four of these are increased in both the user's and producer's accuracy in SOM5. None of the other classifiers could achieve the highest value for both the user's and producer's accuracy for any particular class. It can therefore be concluded that inclusion of a GIS layer as an additional input in the SOM neural network with multi-temporal RADARSAT SAR images improved the accuracy of classification even with only 0.58 % training data.

Table 3 also shows that for some classes user's and producer's accuracy is very low even in SOM5. Considering the mean radar backscattering over time with respect to field information (Fig. 6 and Table 3), it is very clear that the water and built-up area are very distinct classes in the data and lie at the two extremes of the backscattering range in the image. These two classes are well identified in all the classifiers. The rural settlement, mangrove and *B. Aman* classes have similar backscattering at all dates. Inclusion of land-type layer with the images in the SOM network brings out these three classes with better accuracy than other classifier, but *B. Aman* still has very low user's accuracy in SOM5.

Figure 2 indicates that the field polygon over *B. Aman* rice provides a very mixed signature that indicates the limitation of field data in this case. Further, *B. Aman* rice shares the land type (lowlands) with the grass as discussed above in the methodology. Similarly, the shrimp, shrimp & *T. Aman*, *T. Aman* and the unknown class share the same land type class. It can therefore be concluded that the added knowledge of land type in the SOM network was not sufficient to increase the individual class accuracy significantly. Inclusion of further relevant GIS layers in this case may increase the individual class accuracy, and this will be explored in further research.

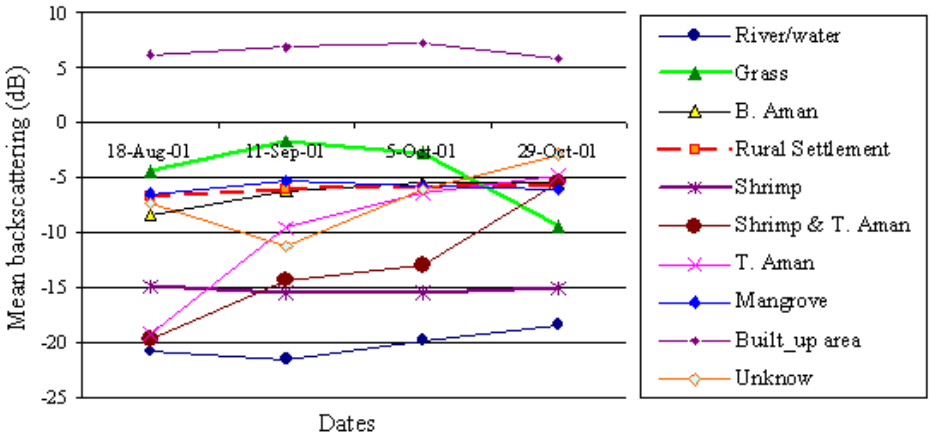

Fig. 6. Mean backscattering plot from different classes over time.

6 CONCLUSION

From the test results it is evident that the incorporation of a GIS layer in the SOM neural network increases the accuracy of the classification with the same amount of training data when compared with the MLH, MHD, and MND classifiers. However, the land type GIS layer may not be the best suited layer in this case. The investigation of the best suited GIS layers for specific tasks is a topic for future research. Also, as the SOM neural network model does not limit the number of input vectors, multiple GIS layers may be considered for further investigation.

In view of the fact that different classifiers perform differently for different classes, it is anticipated that accuracy may be maximised by combining classifiers. In recent years, there has been considerable interest in the problem of combining the outputs of classifiers, as evidenced by the International Workshop on Multiple Classifier Systems series [38]. In general, the design of optimal multiple classifier systems is a computationally hard np-complete problem, the solution of which remains an open question. Future work will be directed towards this issue.

Finally, this is just one case study, which is difficult to generalize from, but it demonstrates that other existing information may be included as an additional layer with remote sensing data in a SOM neural network for improving classification.

Acknowledgments

The authors express sincere gratitude to the Centre for Environment and GIS (CEGIS), Dhaka, Bangladesh for providing with much support relating to the data and fieldwork, and the School of Engineering and Information Sciences, Middlesex University, for providing financial and logistics support for this study.

References

[1] Y. Hara, R. G. Atkins, S. H. Yueh, R. T. Shin, and J. A. Kong, "Application of neural networks to radar image classification," *IEEE Trans. Geosci. Rem. Sens.* **32**(1), 100-109 (1994) [doi:10.1109/36.285193].

[2] EGIS and SPARRSO, "Application of ERS-2 Images in Monitoring Water and Land uses," *Joint publication of Environment and GIS Support Project for Water Sector Planning (EGIS) and Bangladesh Space Research and Remote Sensing Organization (SPSRRSO)*, Bangladesh (2001).

[3] Y. Shao, X. Fan, L. Hao, J. Xiao, S. Ross, B. Brisco, R. Brown, and G. Staples, "Rice monitoring and production estimation using multitemporal RADARSAT," *Rem. Sens. Environ.* **76**(3), 310-325 (2001) [doi:10.1016/S0034-4257(00)00212-1].

[4] H. Hu and Y. Ban, "Urban land-cover mapping and change detection with radarsat sar data using neural network and rule-based classifiers," *Int. Arch. Photogram. Rem. Sens. Spatial Info. Sci.* **37** (Part B7), Beijing (2008).

[5] I. H. Woodhouse, "Stop, look and listen: auditory perception analogies for radar remote sensing," *Int. J. Rem. Sens.* **21** (15), 2901 (2000) [doi:10.1080/01431160050121302].

[6] FAO, *Radar Imagery: Theory and Interpretation*, Remote Sensing Centre, Research and Technology Development Division, FAO, Rome (1993).

[7] B. Brisco and R. J. Brown, "Agriculture application with radar," in *Manual of Remote Sensing*, 3rd ed., Wiley, New York (1998).

[8] M. R. Hord and W. Brooner, "Land-use map accuracy criteria," *Photogram. Eng. Rem. Sens.* **42**, 671-677 (1976).

[9] A. M. Hay, "Sampling designs to test land-use map accuracy," *Photogram. Eng. Rem. Sens.* **45**, 529-533 (1979).

[10] P. J. Curran and H. D. Williamson, "The accuracy of ground data used in remote sensing investigations," *Int. J. Rem. Sens.* **6**, 1637 (1985) [doi:10.1080/01431168508948311].

[11] Q. Zhou and P. Pilesjö, "Improving ground truthing for integrating remotely sensed data and GIS," *Proc. New Developments in Geographical Information Systems*, Int. Soc. Photogram. Remote Sens., Milan, Italy, 30-38 (1996).

[12] S. Brogaard and R. Olafsdottir, "Ground-truths or ground-lies? - Environmental sampling for remote sensing application exemplified by vegetation cover data," *Lund Electronic Reports in Physical Geography*, Dept. Physical Geography, Lund University, Sweden (1997) http://www.lub.lu.se/luft/rapporter/lerpg/1/1Abstract.htm.

[13] J. R. Townshend, "The European contribution to the application of remote sensing to land cover classification," *Int. J. Rem. Sens.* **13**, 1319-1328 (1992) [doi:10.1080/01431169208904193].

[14] G. G. Wilkinson, "Classification algorithms – where next?," in *Soft Computing in Remote Sensing Data Analysis*, pp. 93-99, E. Binaghi., P. A. Brivio, and A. Rampani, Eds., World Scientific, Singapore (1996).

[15] C. H. E. Collet, "Combining spectral and textural features for multispectral image classification with artificial neural networks," *Int. Arch. Photogram. Rem. Sens. Spatial Info. Sci.* **32** (Part 7-4-3 W6), Valladolid, Spain (1999).

[16] G. M. Foody, "Image classification with a neural network: from completely-crisp to fully-fuzzy situation" in *Advances in Remote Sensing and GIS Analysis*, pp. 17-37, P. M. Atkinson and N. J. Tate, Eds., Wiley, West Sussex, UK (1999).

[17] P. M. Mather, *Computer Processing of Remotely-Sensed Images*, Wiley (1987).

[18] F. Roli, G. Giacinto, and G. Vernazza, "Comparison and combination of statistical and neural network algorithms for remote-sensing image classification," in *Neuro-computation in Remote Sensing Data Analysis*, pp. 117-124, I. Kanellopoulos, G. G. Wilkinson, F. Roli, and J. Austin, Eds., Springer, Berlin (1997).

[19] J. A. Benediktsson, P. H. Swain, and O. K. Erosy, "Neural network approaches versus statistical methods in classification of multisource remote sensing data," *IEEE Trans. Geosci. Rem. Sens.* **28**, 540-551 (1990) [doi:10.1109/TGRS.1990.572944].

[20] I. Kanellopoulos, A. Varfis, G. G. Wilkinson, and J. Megier, "Land-cover discrimination in SPOT HRV imagery using an artificial neural network- a 20-class experiment," *Int. J. Rem. Sens.* **13**, 917-924 (1992) [doi:10.1080/01431169208904164].

[21] A. Baraldi and F. Parmiggiani, "A neural network for unsupervised categorisation of multivalued input patterns: an application to satellite image clustering," *IEEE Trans. Geosci. Rem. Sens.* **33**, 305-316 (1995) [doi:10.1109/36.377930].

[22] J. Austin, "High speed image segmentation using a binary neural network," in *Neuro-computation in Remote Sensing Data Analysis*, pp. 202-213, I. Kanellopoulos. G. G. Wilkinson, F. Roli, and J. Austin, Eds., Springer, Berlin (1997).

[23] X. Clastres, M. Samuelides, and G. L. Tarr, "Dynamic segmentation of satellite images using pulsed coupled neural networks," in *Neuro-computation in Remote Sensing Data Analysis*, pp. 160-167, I. Kanellopoulos. G. G. Wilkinson, F. Roli, and J. Austin, Eds., Springer, Berlin (1997).

[24] A. Visa and M. Peura, "Generalisation of neural network based segmentation results for classification purposes," in I., *Neuro-computation in Remote Sensing Data Analysis*, pp. 255-261, I. Kanellopoulos. G. G. Wilkinson, F. Roli, and J. Austin, Eds., Springer, Berlin (1997).

[25] M., E. Petersen, D. de Ridder, H. Handels, "Image processing with neural networks-a review," *Pattern Recog.* **35**, 2279-2301 (2002) [doi:10.1016/S0031-3203(01)00178-9].

[26] S. Cote and A. R. L. Tatnall, "A neural network-based method for tracking feature from satellite sensor images," *Int. J. Rem. Sens.* **16**, 3695-3701 (1995) [doi:10.1080/01431169508954656].

[27] D. T. Pham and E. J. Bayro-Corrochano, "Self-organising neural-network-based pattern clustering method with fuzzy outputs," *Pattern Recog.* **27**, 1103-1110 (1994) [doi:10.1016/0031-3203(94)90148-1].

[28] B. Tso and P. M. Mather, *Classification Methods for Remotely Sensed Data*, Taylor & Francis, London (2001) [doi:10.4324/9780203303566].

[29] M. Torma, "Comparison between three different algorithm," *Photogram. J. Finland* **13**(2), 85-94 (1993).

[30] J. H. Luo and D. C. Tseng, "Self-organizing feature map for multi-spectral spot land cover classification," *Proc. Asian Conf. Rem. Sens.* (2000) http://www.gisdevelopment.net/aars/acrs/2000/ts9/imgp0024.asp

[31] E. Merenyi, J. V. Taranik, T. Minor, and W. H. Farrand, "Quantitative comparison of neural network and conventional classifiers for hyperspectral imagery," in *Summaries 6th Annual JPL Airborne Earth Sci. Work.*, Vol. 1, Pasadena, CA(1996).

[32] FAP19/ISPAN, *Satellite-based radar for flood monitoring in Bangladesh*, Flood Action Plan 19, Ministry of Water Resources, Bangladesh, Dhaka (1995).

[33] D. T. Kuan, A. A. Sawchuk, T. C. Strand, and P. Chavel, "Adaptive restoration of images with speckle," *IEEE Trans. Acoust., Speech Signal Process.* **35**(3), 373-383 (1987) [doi:10.1109/TASSP.1987.1165131].

[34] EGIS, *Mapping and Monitoring Floods with RADARSAT Images*, Environmental and GIS Support Project for Water Sector Planning/Delft Hydraulis, Water Resources Planning Organization (WARPO), Ministry of Water Resources, Bangladesh (1997)

[35] ISPAN, *Bangladesh National Level GIS Database*, Bangladesh Flood Action Plan, Irrigation Support Project for Asia and the Near East (ISPAN), Bangladesh, pp. 23-26 (1995).

[36] MPO, *Agricultural Production System*, **14**, *Master Plan Organisation (MPO)*, Ministry of Irrigation, Water Development and Flood Control, Government of Bangladesh (1987).

[37] T. Kohonen, *Self-Organizing Maps*, Springer, Berlin (1995).

[38] J. A. Benediktsson, J. Kittler, and F. Roli, Eds., *Multiple Classifier Systems, Proc. 8th Int. Work. Multiple Classifier Syst., Reykjavik, Iceland*, Springer, Berlin(2009).